

# International Journal of Applied Mathematics in Control Engineering

Journal homepage: <http://www.ijamce.com>

## Load Feedback-Based Obstacles Traversing Locomotion for a Serpentine Robot

Jinru Man, Xingguo Song<sup>\*</sup>, Rahman Md Azizur, Abu Nasher Md Nazibullah*Mechanical Engineering School, Southwest Jiaotong University, Chengdu 610031, China*

### ARTICLE INFO

## Article history:

Received 5 February 2024

Accepted 13 April 2024

Available online 15 April 2024

## Keywords:

Serpentine robot

Load feedback

Angle adaptive control

Cross obstacles

### ABSTRACT

When serpentine robots move in the complex and unstructured environment, collisions between the serpentine robot and obstacles often impede its movement. In this paper, the robot utilizes collisions between the serpentine robot and obstacles to change robot's trajectory, or relies on obstacles to guide the locomotion of the serpentine robot. An angle adaptive control based on load feedback is proposed for local gait planning of robots. When the robot joint load exceeds the set threshold, the joint angle is adjusted in time to adapt to terrain changes. Experiments are conducted to cross different obstacles using different control methods, and comparisons are made in terms of energy loss and motion rate. The experimental results show that this gait has the lowest energy consumption while ensuring the robot's motion rate.

Published by Y.X.Union. All rights reserved.

## 1. Introduction

With its slender body structure and flexible movement, the biological snake is able to rely on limbless joints to contact the environment to perceive information (Schiebel et al., 2019), and control the joints to adapt to the nearby terrain based on the information fed back to cross narrow ditches and enter hollows. It is highly adaptable to complex unstructured terrain and can enter unknown environments that are difficult for humans to reach. The snake's main mode of movements include lateral undulation (Gans, 1962), rectilinear locomotion (Jayne, 2020), sidewinding locomotion (Clark & Summers, 2009; Astley et al., 2015) and concertina locomotion (Jayne & Davis, 1991) and so on. Lateral undulation is the most common form of movement for snakes in nature. Lateral undulation uses continuous slithering of the body to contact the environment and thus propel the body (Gans, 1962), which is the most energy-efficient way to move in open areas. However, lateral undulation is not suitable for smooth, low-friction surfaces and narrow passages. If the serpentine robot has the multi-sport approach of snakes, it can use limbless joint contacts to perceive environmental information in order to control the joints to adapt to unknown terrain environments. Unlike wheeled and footed robots, snake robots' movements are more diverse and flexible, capable of accomplishing behavioral control such as lateral undulation, rectilinear locomotion, sidewinding locomotion, climbing over obstacles (Tanaka et al., 2020)

and climbing columns (Rollinson & Choset, 2013, 2016), it can be applied in complex terrain environments which are inaccessible to humans. However, current snake robots mostly plan the robot's gait based on the global known environment, and it is difficult to simulate the behavior of snakes to adapt to unknown complex terrain.

To enable the snake robot to adapt to unknown obstacles terrain, some scholars used vision to identify obstacles in the surrounding environment by equipping the camera on the robot. Then the snake robot will perform trajectory planning, and the robot's gait commands are constantly and dynamically adjusted while travelling obstacles, thus the snake robot is guided to avoid obstacles. Li et al. (2020) have used two vision cameras, one mounted on the head of the snake robot for target recognition and the other is an overhead camera which is responsible for robot localization and identification of surrounding obstacles, the robot is able to follow planned paths for target exploration. Tanaka et al. (2015) have used distance sensors installed on the robot's whole-body joints to detect obstacles around the robot and combined them with SLAM to achieve obstacle avoidance. Bing et al. (2017) have guided the robot for target tracking by vision sensors mounted on the head module. Chang et al. (2018) have developed a lateral undulation dynamics model and proposed an optimal control trajectory synthesis strategy and a closed-loop feedback control approach to trajectory tracking for the robot to navigate to a specified target location in an arbitrary obstacle environment. Chang et al. (2020) have developed a snake robot with traveling wave rectilinear gait, which can correct gait commands by

\* Corresponding author.

E-mail addresses: [xg.song@hotmail.com](mailto:xg.song@hotmail.com) (X. Song)Digital Object Identifiers: <https://doi.org/10.62953/IJAMCE.547538>

capturing the position of the robot and obstacles through a top camera, avoiding obstacles and reaching the target point. Then the top camera is removed, and only the environment images of each gait cycle is captured by the wireless monocular head camera of the snake robot platform for self-positioning and dynamic planning (Chang et al., 2019a). However, using SLAM for obstacle avoidance creates inflation layers for obstacles that are considered impenetrable layers. When the robot faces narrow obstacles which it should be able to traverse but cannot travel through. In addition, some researchers have added force sensors to the joints of snake robots to propel the snake robot forward according to the magnitude and direction of the reaction force of obstacles on the robot joints (Jia & Ma, 2020; Kano et al., 2011; Transteth et al., 2008; Hanssen et al., 2020). Liljebäck et al. (2009, 2010a, 2010b, 2011) have designed a snake robot with a smooth surface and spherical joints capable of measuring contact forces, and developed a hybrid dynamics model of a planar snake robot interacting with obstacles so that the snake robot can use obstacles in its path as push points to propel itself forward while avoiding obstacles that interfere with its locomotion (obstacle-aided locomotion). This approach necessitates the installation of many force sensors in the robot shell, and the different angles of installation will also affect the accuracy of contact force measurement and joint posture solution. The process of solving the data is also more complex and needs to run on a CPU with higher computing power.

A number of studies have also focused on the design of motion pattern control for snake robots. Wu et al. (2013) have established a motion pattern for head navigation based on the neural controller of the central pattern generator (CPG), which can control the head of the snake robot to maintain the same direction of motion. The sensors can accurately detect obstacles ahead to avoid collisions. In addition, shape-based complaint control has been used in some studies to use robot compliance to facilitate robot locomotion in complex terrain (Whitman et al., 2016; Travers et al., 2016, 2018). Sartoretti et al. (2021) have constructed a decentralized shape control framework and added a continuous steering controller. The robot can navigate autonomously in dense environments. After that, a depth camera is equipped in the head, so that the robot could select the move direction based on visual feedback. However, the camera occupies a relatively large space, and the robot's CPU is required to have high algorithm power. These methods require the snake robot to be paired with a computer capable of running complex algorithms, or connected to the computer through long data cables, which can result in a significant increase in the size of the snake robot and limited movement space.

In this paper, we design a small and low-cost serpentine robot that can autonomously travel in different obstacle environments, in order to improve the adaptability and stability of the serpentine robot in crossing obstacles in unknown terrain. It can perceive the unknown terrain environment and use the information fed back to continuously adjust and plan the robot's gait, thus the robot can cross the unknown obstacles. Based on the robot's interaction with obstacles in the environment, we design an angle adaptive control based on load feedback for local adjustment of the joint posture, which reduces the probability of the robot getting stuck while crossing narrow obstacles. The experiment has demonstrated the superiority of our proposed method in terms of robot energy loss and motion rate.

## 2. Problem Description

### 2.1 Serpentine robot design

As shown in Fig 1, the robot consists of a head module, 14 joint

modules and 112 passive wheels. The robot body length is about 775mm, width and height are 55mm. The robot adopts a modular design with the same structure of all joint modules except the head module, which makes it easy to increase or decrease the number of joints and improves the flexibility of the robot. We select the Dynamixel XL series motor, the XL-320, as the joint actuator for the robot, with a torque of 0.39 Nm and a relatively small size to facilitate lightweight design of the robot for crossing narrow obstacles. The microcontroller OpenCM9.04 receives control signals from the PC via the Bluetooth module, parses them and sends the control commands of the target motors to the motors. All the motors coordinate to complete the robot locomotion gait. At the same time, the microcontroller receives real-time information about the angle and load of the joint motors and the microswitches during the robot locomotion.

The robot joint modules are connected to each other in an orthogonal way, i.e., the drive axes of adjacent joints are perpendicular to each other. The joint modules alternate as yaw joints and pitch joints to produce horizontal and vertical plane rotation, respectively, and the joint angle rotation range is set from  $-90^\circ$  to  $90^\circ$ , where the yaw joints and pitch joints are both seven. The mutually orthogonal connection gives the robot the ability to move in three dimensions. Compared with the universal connection method, the orthogonal connection has the advantages of simple structure, low cost and simple control. The motors of the robot in the previous work (Tanaka et al., 2020; Chang et al., 2019b; Chen et al. 2018; Luo et al., 2018) are also connected by orthogonal connections, but their orthogonal connections are fixed and cannot be changed. In contrast, our robot joint modules can be converted from the orthogonal connection to the parallel connection. Also, the joint modules have three more joints than they do, so that the robot has more joints to rotate to provide forward thrust when moving, and the robot is less likely to get stuck when crossing obstacles with narrower spacing. Each plane of the robot joint module uses the passive wheel structure. When the robot's perimeter is in contact with the obstacle, the rolling of the passive wheel also reduces the friction between the robot and the obstacle, making the robot more fluid in crossing obstacles.



Fig. 1. A small serpentine robot and its joint module design.

### 2.2 Lateral undulation as robot locomotion gait

By simulating the way that the lateral friction is greater than the tangential friction generated by the scales of a snake and thus slithers forward, the robot adopts a passive wheel design in which lateral friction and tangential friction are sliding friction and rolling friction respectively. The lateral friction force is greater than the tangential

friction force, so that the robot can achieve lateral undulation.

Hirose (1993) proposed a serpenoid curve that mimics the lateral undulation of biological snakes by observing the motion pattern of biological snakes, its curvature equation is given by:

$$k(s) = -\frac{2K_n\pi\alpha_0}{L}\sin\left(\frac{2K_n\pi}{L}s\right) \quad (1)$$

where  $s$  is the arc length between a point on the serpentine curve and the starting point,  $L$  is the total body length of the snake robot,  $K_n$  is the number of body waves contained in the snake robot, and  $\alpha_0$  is the initial angle of the serpentine curve.

The serpentine robot locomotion gait is essentially a time-varying curve of the robot joints, and its state variable  $\Phi(t) = (\Phi_1(t), \Phi_2(t), \dots, \Phi_N(t)) \in \mathbf{R}^N$  represents the joint angle of the robot at moment  $t$ . Equation (1) for a discrete approximation of a snake robot with the number of joints  $N$ , the joint angle function of its lateral undulation gait can be obtained as:

$$\Phi_i(t) = A \sin(\omega t + (i-1)\delta) + \Phi_0 \quad (2)$$

where  $i \in \{1, 2, \dots, N\}$ ,  $N$  is the total number of robot joints,  $A$  is the amplitude of the serpenoid curve, which determines the degree of bending of the robot's body during locomotion;  $\omega$  is the temporal frequency, which determines how fast or slow the body oscillates during robot locomotion;  $\delta$  is the angular phase difference between adjacent joints, which determines the number of robot body waves;  $\Phi_0$  is the joint offset, which can change the forward direction of the robot.

In this paper, the time-varying continuous backbone curve for fitting the robot's locomotion gait can be decomposed into two planes of time-varying body wave components on the horizontal and vertical planes of the locomotion surface. Our robot joints are in orthogonal mode, and the horizontal component of the robot discrete model to the continuous time-varying locomotion body curve is the yaw joint trajectory of the odd IDs, and then the vertical component of the continuous time-varying body curve is the pitch joint trajectory of the even IDs.

For lateral undulation, the trajectory occurs only in the horizontal, so it is sufficient to define the body wave component in the plane where no locomotion is generated as zero. Only the yaw joint is rotated, while the pitch joint angle is zero. The joint angle control function for lateral undulation can be obtained for the number of robot joints in this study as follows:

$$\begin{cases} \theta_i(t) = A_e \sin(\omega_e t + \frac{(N-i-1)}{2}\delta_e) + \theta_{e0} \\ \theta_j(t) = 0 \end{cases} \quad (3)$$

where  $\theta_i(t)$  is the joint angle of the  $i$ -th joint of the robot, i.e., the yaw joint trajectory of the odd IDs,  $i \in \{1, 3, \dots, N-1\}$ ,  $\theta_i(t)$  is the joint angle of the  $j$ -th joint of the robot, i.e., the pitch joint trajectory with even IDs,  $j \in \{2, 4, \dots, N\}$ .  $A_e$  is the amplitude of the yaw joint,  $\omega_e$  is the temporal frequency of yaw joint rotation,  $\delta_e$  is the angular phase difference of the yaw joint,  $\theta_{e0}$  is the offset of the yaw joint. The shape of lateral undulation can be adjusted by these parameters. By adding a joint offset to the gait curve of the horizontal body wave component, the symmetric centerline of the joint angle can be shifted away from the zero position by the specified offset, thereby changing the forward direction of the robot.

Horizontal body wave component propagates from the head to the tail of the robot, using the transverse friction of the passive wheel is greater than the tangential friction to propel the robot forward locomotion. The horizontal and vertical body wave components of

the lateral undulation are shown in Fig. 2.

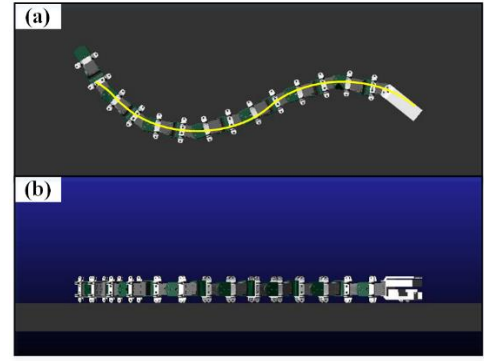


Fig. 2. Serpentine robot lateral undulation gait. (a) Horizontal body wave component in the top view. (b) Vertical body wave component in side view.

### 3. Angle adaptive control based on load feedback

When the serpentine robot travels obstacle environment, we simplify the joint mechanics model when colliding with an obstacle and set the coupling force of the front and rear joints of the target joint to its known force, only consider the simplified mechanical model when a single joint collides with an obstacle. The joint forces are shown in Fig. 3, where  $f_{cf}$  and  $f_{cr}$  are the coupling forces on the current joint caused by the rotation of the front and rear joints respectively, assuming that the action is on the front and rear joint axes respectively.  $T$  is the joint output torque.  $f_e$  is the reaction force applied to the joint in contact with the obstacle.

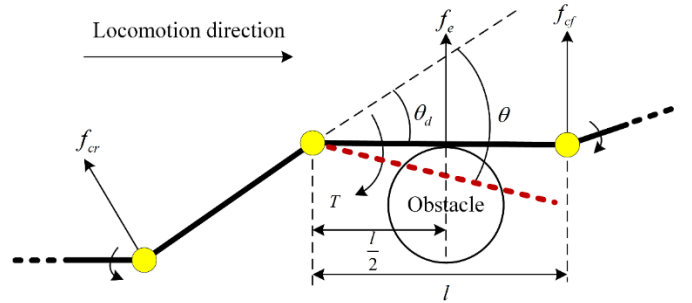


Fig. 3. Force on single joint of the robot in contact with an obstacle, the red dashed line is the target position of the joint rotation.

$$T_e = \frac{l}{2} f_e \quad (4)$$

$$T_c = (f_{cf} - f_{cr})l \quad (5)$$

Assuming that the total coupling force on the joint is  $f_c$ , i.e.,  $f_c = f_{cf} - f_{cr}$ , then the condition for the equilibrium of the joint forces is:

$$T = T_e + T_c = l(f_c + \frac{f_e}{2}) \quad (6)$$

In order for the motors to reach the target angle  $\theta$ , the joint output torque  $T$  is continuously increased, which leads to overload of the joint motor and damage to the motor. To avoid this situation, the target angle of the joint needs to be made to converge to the desired angle  $\theta_d$ . In this case, motion regulator is needed to change the target angle  $\theta$  to  $\theta_d$  through a series of calculations and send it to the joint controller. In the joint trajectory control of the serpentine robot, the task of motion regulator should focus on the transformation relationship between  $\theta$  and  $\theta_d$ .

$F$  is the driving force of the robot joint,  $m$  is the inertial mass, then the equation of mass motion of a single joint can be written as:

$$m\ddot{\theta} = F + f_c + f_e \quad (7)$$

The control of the joint motor of the serpentine robot is angle adjustment. The joints need to overcome the coupling force  $f_c$  of adjacent joints in front and behind to rotate to the target position without external force. Its angle adjustment can be expressed in a PD controller as follows:

$$F + f_c = k_p(\theta_d - \theta) - k_d(\dot{\theta} - \dot{\theta}_d) \quad (8)$$

where  $k_d$  and  $k_p$  is the positive gain. Bringing Equation (8) into Equation (7) yields a simplified dynamics model of the serpentine robot system with  $N$  joints in interacting with the environment:

$$m\ddot{\theta} + k_d(\dot{\theta} - \dot{\theta}_d) + k_p(\theta - \theta_d) = f_e \quad (9)$$

The joint desired angle  $\theta_d$  can be varied according to the external force  $f_e$ . The motion regulator sets the target angle  $\theta$  of the joint. When no external force is applied to the joint,  $f_e = 0$ , then the joint desired angle converges to the target angle, i.e.,  $\theta_d = \theta$ . When the joint is subjected to external forces,  $f_e$  is not zero, the joint desired angle varies according to the magnitude of the external force.

In this work, the external forces on the robot joints from the obstacles are not measured by installing force sensors on the robot. Rather, it is indirectly reflected by the load placed on the joint. The joint motor used by the robot has the function of feeding back the current load on the joint. It is important to note that, the current joint load is an inferred value based on its internal output value. Therefore, the external force applied to the joint cannot be measured precisely, but the direction and magnitude of the external force applied to the joint can be predicted, which can equivalently reflect the forces on the robot in an obstacle environment. From Equation (6), it is obtained as:

$$f_e = 2\left(\frac{T}{l} - f_c\right) \quad (10)$$

In the case where the joint coupling force  $f_c$  is known, the external force can be obtained from the joint load  $f_e$ . Since the load feedback of the joint motor is inferred from the joint torque, the load feedback of the joint motor can be mapped to the external force applied to the joint according to Equation (10).

The joint motor gives feedback on the current load value  $L_p$  being applied. The joint coupling force  $f_c$  is set to a threshold value and mapped to the joint load  $L_c$ . If  $L_p \leq L_c$ , then the joint is not subjected to external forces. If  $L_p > L_c$ , then the joint is subjected to an external force. The current joint angle is detected and the desired angle  $\theta_d$  for interaction with the obstacle is calculated. Using the above control based on load feedback makes the joint target angle  $\theta$  converge to the desired angle  $\theta_d$ . When the robot encounters the obstacles which is difficult to cross and the robot's joint trajectory cannot reach a predetermined value, this method optimizes the forced joint trajectory according to the force of the obstacle, avoiding the robot joints getting stuck in obstacles.

Fig. 4 and Fig. 5 shows a trial to test the effectiveness of this load feedback control. Firstly, we pre-set the shape of the robot as a sine function waveform that does not change with time. Subsequently, by manually applying tension to both ends of the robot, the robot is simulated to be subjected to significant obstacle forces when crossing complex environments. The plot in Fig. 4 shows the initial shape of the robot at the moment  $t = 0s$ . Fig. 5 shows that applying an external force to the robot at  $t = 2s$  causes the yaw joint angle to gradually decrease and the load to gradually increase. At  $t = 3s$  the robot adjusts its form to a straight line according to the load feedback to adapt to the change in external force. Removing the external force at  $t = 4s$ , the joint angle and load gradually return to the stable value at the

beginning. At  $t = 6s$  the shape of the robot returns to the state before the external force is applied.

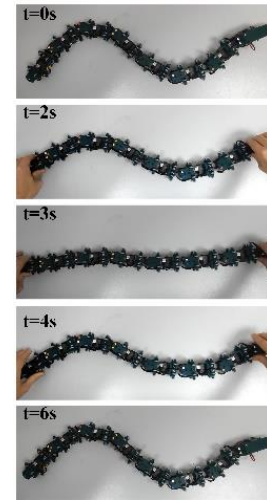


Fig. 4. The state of the robot at different times after being subjected to the external force.

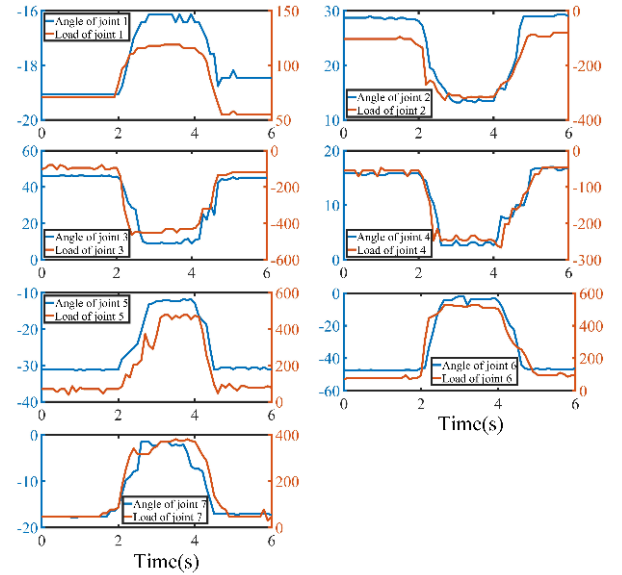


Fig. 5. The yaw joint angle and load.

## 4. Experimental Details

### 4.1 Experimental Setup

The ground for each experiment uses the foam mats. Obstacles are made by 3D printing and then placed. We place the serpentine robot outside the obstacle environment. The host computer sends locomotion commands to the robot via the Bluetooth module to start it moving towards the obstacle environment. The camera is placed above the obstacle environment to take top view video. The gait of the robot in the experiment is lateral undulation. The initial values of the gait parameters are the same and constant for each experiment. Tab. 1. defines the gait parameters of the horizontal body wave component, i.e., the yaw joint. For subsequent analysis and processing of the data, the angle and load information of the joint motors during robot motion is transmitted back to the host computer via Bluetooth in real time.



**Tab. 1.** Yaw joint gait parameters.

Descriptions	Symbols	Values
Amplitude	$A_e$	$2\pi/9$
Temporal frequency	$\omega_e$	$\pi$ rad/s
Angular phase difference	$\delta_e$	$2\pi/9$ rad

#### 4.1 Robot environments and analysis

To verify the advantages of the method proposed in the previous section for the robot locomotion in different unknown terrain environments, we conducted multiple experiments of travelling obstacles in the following two obstacle environments: (1) travelling the cylindrical obstacles; (2) contacting with the vertical plane obstacle. The robot utilizes lateral undulation gait, and uses two different control methods in two different terrain environments in turn: (A) open-loop control without load feedback, (B) closed-loop control based on load feedback. To evaluate the benefits of angle adaptive control based on load feedback for the locomotion of the snake robot in obstacle environments, the data collected from the experiments are compared and analyzed, and the locomotion efficiency of the snake robot is observed when travelling the unknown obstacle environment.

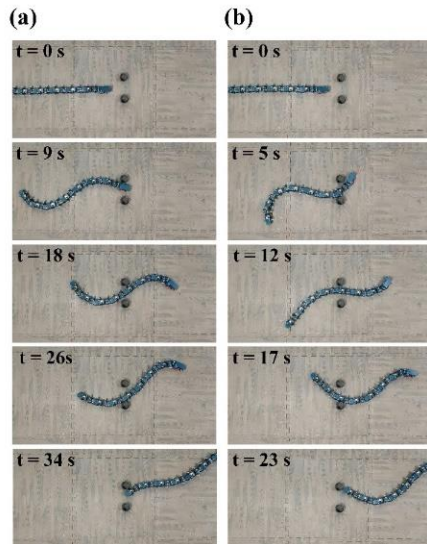


**Fig. 6.** Comparison of two control methods used by the robot to cross the cylindrical obstacles, time moves from top to bottom: (a) open-loop control without load feedback, (b) closed-loop control based on load feedback.

Cylindrical obstacles are set up on the foam mats with cylindrical radius  $r = 25\text{mm}$ . The columns are aligned in a direction perpendicular to the motion direction of the robot with a center distance of  $d = 130\text{ mm}$ . Fig. 6 shows the progress of the robot's motion cross the cylindrical obstacle using each of the two control methods. Fig. 7 shows the angle and load data for selected second, fourth, and sixth yaw joints. It can be seen that with method (A), the robot can rely on the thrust generated by the swinging of the joints at the back to move forward and cross obstacles, but the method can't adjust the joint angles, which leads to excessive loads, increased energy consumption, and slow movement speed.

Using method (B), the joints that interact with the obstacles during robot motion are adapted to the obstacles by reducing their angles and joint loads by angle adaptive control. The joints that are not interacting with the obstacle generated forward propulsion in a set waveform to push the joints in the obstacle forward, and so on until the whole robot travel the obstacle terrain. But the gait of the collision

is not planned in advance for the rear joints.

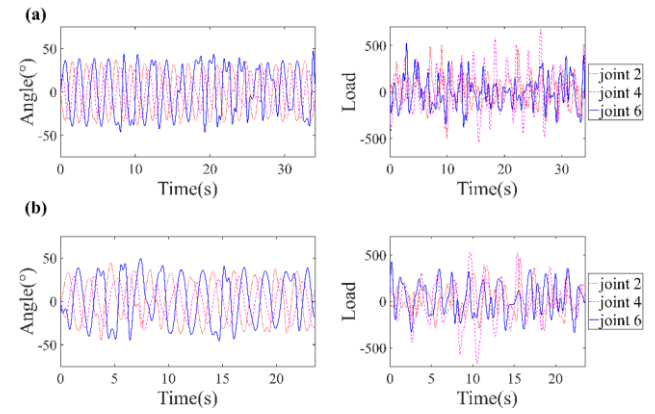


**Fig. 7.** Joint angles and loads of the second, fourth, and sixth yaw joints of the robot cross cylindrical obstacles under two control methods: (a) open-loop control without load feedback, (b) closed-loop control based on load feedback.

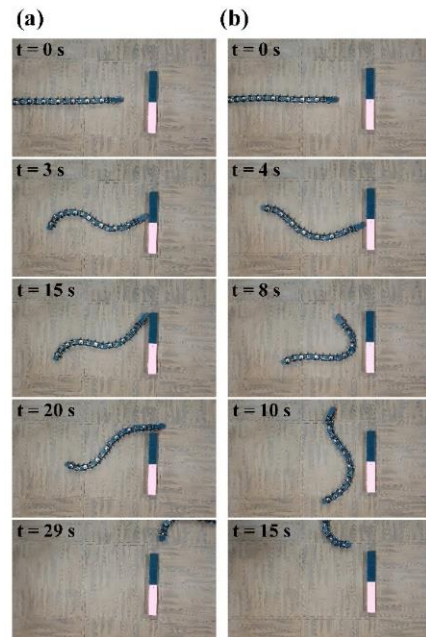


**Fig. 8.** Comparison of two control methods used by the robot in collision with the vertical plane obstacle, time moves from top to bottom: (a) open-loop control without load feedback, (b) closed-loop control based on load feedback.

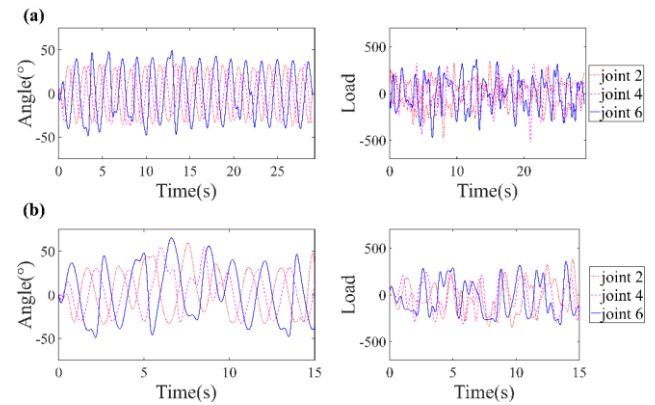


**Fig. 9.** Joint angles and loads of the second, fourth, and sixth yaw joints of the robot during colliding with the vertical plane obstacle under two control methods: (a) open-loop control without load feedback, (b) closed-loop control based on load feedback.

A vertical plane obstacle is set up in the forward direction of the robot, and the height of the obstacle is slightly higher than the height of the robot, in order to reach the effect of simulating the collision between the robot and the wall obstacle. Fig. 8 depicts the motion of the robot before and after a collision with a vertical plane obstacle. Fig. 9 shows the angle and load data for the second, fourth, and sixth yaw joints of the robot in this environment. With method (A), due to the sideways movement of the passive wheels, the robot is deflected after a sustained collision and continues to move in that direction. However, during the process the robot joints keep violently colliding with the obstacle resulting in excessive loads, high energy consumption and unstable motion. Using method (B), the effect is similar to that of method (A), but the robot joints can adjust the joint angles appropriately according to the load feedback.

## 5. Conclusion

In this paper, we studied the locomotion gait for the serpentine robot to cross unknown obstacles by sensing the environment, and experimentally validated it with the robot platform in a variety of different obstacle environments. We proposed an angle adaptive control based on load feedback. When the local joints of the robot are in contact with obstacles, they can dynamically adjust the size of the joint angle to accommodate changes in the local terrain depending on the amount of load on the joint. The experiment verified that the gait enables the robot to adapt to different terrain environment changes, which improves the robot's motion efficiency cross obstacles and reduces motion energy consumption.

In the future, we will use the load-feedback based control in the pitch joints, the robot can adjust its posture to adapt to changes in three-dimensional rugged terrain.

## Acknowledgements

This work is supported by the Fundamental Research Funds for the Central Universities (No. 2682022KJ015), State Key Laboratory of Robotics and Systems (HIT) (SKLRS-2020-KF-13).

## References

- Astley, H. C., Gong, C., Dai, J., Travers, M., Serrano, M. M., Vela, P. A., ... & Goldman, D. I., 2015. Modulation of orthogonal body waves enables high maneuverability in sidewinding locomotion. *Proceedings of the National Academy of Sciences*, 112(19), 6200-6205.
- Bing, Z., Cheng, L., Huang, K., Jiang, Z., Chen, G., Röhrbein, F., & Knoll, A., 2017, September. Towards autonomous locomotion: Slithering gait design of a snake-like robot for target observation and tracking. In 2017 IEEE/RSJ International Conference on Intelligent Robots and Systems (IROS), pp. 2698-2703.
- Chang, A. H., Hyun, N. S. P., Verriest, E. I., & Vela, P. A., 2018, June. Optimal trajectory planning and feedback control of lateral undulation in snake-like robots. In 2018 Annual American Control Conference (ACC), pp. 2114-2120.
- Chang, A. H., Feng, S., Zhao, Y., Smith, J. S., & Vela, P. A., 2019a. Autonomous, monocular, vision-based snake robot navigation and traversal of cluttered environments using rectilinear gait motion. *arXiv preprint arXiv:1908.07101*.
- Chang, A. H., & Vela, P. A., 2019b. Evaluation of bio-inspired scales on locomotion performance of snake-like robots. *Robotica*, 37(8), 1302-1319.
- Chang, A. H., & Vela, P. A., 2020. Shape-centric modeling for control of traveling wave rectilinear locomotion on snake-like robots. *Robotics and Autonomous Systems*, 124, 103406.
- Chen, J., et al., Stability Discrimination of Quadruped Robots by Using Tetrahedral Method. *International Journal of Applied Mathematics in Control Engineering*, 2018. 1(2): p. 165-171.
- Clark, A. J., & Summers, A. P., 2009. Serpentine steps. *Nature*, 459(7249), 919-920.
- Gans, C., 1962. Terrestrial locomotion without limbs. *American Zoologist*, 2(2), 167-182.
- Hanssen, K. G., Transth, A. A., Sanfilippo, F., Liljebäck, P., & Stavdahl, Ø., 2020, September. Path Planning for Perception-Driven Obstacle-Aided Snake Robot Locomotion. In 2020 IEEE 16th International Workshop on Advanced Motion Control (AMC), pp. 98-104.
- Hirose, S., 1993. *Biologically Inspired Robots: SnakeLike Locomotors and Manipulators*. Oxford: Oxford University Press.
- Jayne, B. C., & Davis, J. D., 1991. Kinematics and performance capacity for the concertina locomotion of a snake (*Coluber constrictor*). *Journal of Experimental Biology*, 156(1), 539-556.
- Jayne, B. C., 2020. What defines different modes of snake locomotion?. *Integrative and comparative biology*, 60(1), 156-170.
- Jia, Y., & Ma, S., 2020, October. A bayesian-based controller for snake robot locomotion in unstructured environments. In 2020 IEEE/RSJ International Conference on Intelligent Robots and Systems (IROS), pp. 7752-7757.
- Kano, T., Sato, T., Kobayashi, R., & Ishiguro, A., 2011, May. Decentralized control of scaffold-assisted serpentine locomotion that exploits body softness. In 2011 IEEE International Conference on Robotics and Automation, pp. 5129-5134.
- Li, G., Waldum, H. B., Grindvik, M. O., Jørundl, R. S., & Zhang, H., 2020. Development of a vision-based target exploration system for snake-like robots in structured environments. *International Journal of Advanced Robotic Systems*, 17(4), 1729881420936141.
- Liljebäck, P., Fjerdingen, S., Pettersen, K. Y., & Stavdahl, O., 2009, May. A snake robot joint mechanism with a contact force measurement system. In 2009 IEEE International Conference on Robotics and Automation, pp. 3815-3820.
- Liljebäck, P., Pettersen, K. Y., & Stavdahl, Ø., 2010a, May. A snake robot with a contact force measurement system for obstacle-aided locomotion. In 2010 IEEE international conference on robotics and automation, pp. 683-690.
- Liljebäck, P., Pettersen, K. Y., Stavdahl, Ø., & Gravdahl, J. T., 2010b. Hybrid modelling and control of obstacle-aided snake robot locomotion. *IEEE Transactions on Robotics*, 26(5), 781-799.
- Liljebäck, P., Pettersen, K. Y., Stavdahl, Ø., & Gravdahl, J. T., 2011. Experimental investigation of obstacle-aided locomotion with a snake robot. *IEEE Transactions on Robotics*, 27(4), 792-800.
- Luo, X., et al., Time Delay Estimation-based Adaptive Sliding-Mode Control for Nonholonomic Mobile Robots. *International Journal of Applied Mathematics in Control Engineering*, 2018. 1(1): p. 1-8.
- Rollinson, D., & Choset, H., 2013, May. Gait-based compliant control for snake robots. In 2013 IEEE International Conference on Robotics and Automation, pp. 5138-5143.
- Rollinson, D., & Choset, H., 2016. Pipe network locomotion with a snake robot. *Journal of Field Robotics*, 33(3), 322-336.
- Sartoretti, G., Wang, T., Chuang, G., Li, Q., & Choset, H., 2021, May. Autonomous decentralized shape-based navigation for snake robots in dense environments. In 2021 IEEE International Conference on Robotics and Automation (ICRA), pp. 9276-9282.
- Schiebel, P. E., Rieser, J. M., Hubbard, A. M., Chen, L., Rocklin, D. Z., & Goldman, D. I., 2019. Mechanical diffraction reveals the role of passive dynamics in a slithering snake. *Proceedings of the National Academy of Sciences*, 116(11), 4798-4803.
- Tanaka, M., Kon, K., & Tanaka, K., 2015. Range-sensor-based semiautonomous whole-body collision avoidance of a snake robot. *IEEE Transactions on Control Systems Technology*, 23(5), 1927-1934.
- Tanaka, M., Nakajima, M., Ariizumi, R., & Tanaka, K., 2020. Three-dimensional steering for an articulated mobile robot with prismatic joints with consideration of hardware limitations. *Advanced Robotics*, 34(11), 767-779.
- Transth, A. A., Leine, R. I., Glocker, C., Pettersen, K. Y., & Liljebäck, P., 2008. Snake robot obstacle-aided locomotion: Modeling, simulations, and experiments. *IEEE Transactions on Robotics*, 24(1), 88-104.
- Travers, M. J., Whitman, J., Schiebel, P. E., Goldman, D. I., & Choset, H., 2016, June. Shape-Based Compliance in Locomotion. In *Robotics: Science and Systems*. Vol. 12.
- Travers, M., Whitman, J., & Choset, H., 2018. Shape-based coordination in locomotion control. *The International Journal of Robotics Research*, 37(10), 1253-1268.
- Whitman, J., Ruscelli, F., Travers, M., & Choset, H., 2016, December. Shape-based compliant control with variable coordination centralization on a snake robot. In 2016 IEEE 55th Conference on Decision and Control (CDC), pp. 5165-5170.

Wu, X., & Ma, S., 2013. Neurally controlled steering for collision-free behavior of a snake robot. IEEE Transactions on Control Systems Technology, 21(6), 2443-2449.



**Jinru Man** is currently a graduate student in the School of Mechanical Engineering at Southwest Jiaotong University and his research interest is in environment adaptive control of bionic snake robots.



**Xingguo Song**, Ph.D., graduated from Harbin Institute of Technology, School of Mechanical and Electrical Engineering, majoring in Mechanical Design and Theory, is a visiting scholar at Rice University and a postdoctoral fellow at Johns Hopkins University, USA. His main research interests are intelligent robotics, UAV path planning, bionic robotics, and computer vision.



**Rahman Md Azizur**, a graduate student at Southwest Jiaotong University's School of Mechanical Engineering, research interest: specializes in bionic snake robots, study the kinematic model and dynamic model of the manipulator, study the motion planning algorithm of the manipulator.



**Abu Nasher Md Nazibullah**, a graduate student at Southwest Jiaotong University's School of Mechanical Engineering, specializes in bionic snake robots. Their research focuses on environment adaptive control, driven by a passion for nature-inspired innovation in robotics.